Thermomagnetic recording stability of taenite-containing meteoritic cloudy zones

José A. P. M. Devienne[1], Thomas A. Berndt[1], Wyn Williams[2], Lesleis Nagy[3]

[1]Department of Geophysics, School of Earth and Space Sciences, Peking University, Beijing 100871, PR China
[2]School of GeoSciences, The University of Edinburgh, Edinburgh, EH9 3FE, UK
[3]Department of Geophysics, Ocean and Ecological Sciences, University of Liverpool, Liverpool, L697ZE, UK

Key Points:

- Nanometer-sized taenite present in meteoritic cloudy zone is likely to preserve stable magnetization states
- The island sizes of most fast cooled meteorites coincides with the range in which stable single domain (SD) taenite forms
- Stable SD configurations are possibly preserved during tetrataenite ordering

Corresponding author: J. Devienne, `devienne@stu.pku.edu.cn`

Abstract

The cloudy zone (CZ), a nm-sized intergrowth of taenite or tetrataenite crystals (or islands), is the most promising phase to preserve palaeomagnetic records in (stony-)iron meteorites. While slowly-cooled meteorites form tetrataenite – an extremely good recorder – fast-cooled meteorites contain fine-grained taenite islands, which were considered unsuitable for palaeomagnetic studies. In this work, however, we show that nm-sized taenite grains are stable over billion-year timescales, indicating that taenite-bearing meteorites are reliable sources of paleomagnetic information. Additionally, we find a range of sizes for which taenite forms stable single-domain structures. Single-domain states might be preserved even through subsequent tetrataenite ordering, implying that tetrataenite might carry magnetization state inherited from its precursor taenite. This remanent magnetization can be up to 10^5 years older than that of larger tetrataenite islands in the same meteorite, which would have been reset upon ordering. This allow studding to two distinct events of planetesimal formation from a single sample.

Plain Language Summary

Metallic meteorites are fragments of small planetary bodies that formed during the first million years of our solar system. They can provide a wealth of information about how small planets form, how they undergo differentiation and whether (and how) they once had a liquid core capable of generating self-driven magnetic fields. The presence of a planetary magnetic field is ultimately a necessary ingredient for evolution of life, as without a strong field, microorganisms would be exposed to deadly cosmic rays, and any atmosphere would be prone to being blown away by solar wind - a fate that happened to Mars millions of years ago. Recent works have shown that nanometer-sized tetrataenite grains present in slowly cooled meteorites are able to preserve records of ancient magnetic activity of their parent bodies. In this work we show that taenite, a common magnetic mineral in fast cooled meteorites, is also capable of reliably preserving records of ancient magnetic fields. These results open a window of opportunity in using metallic meteorites, in particular the so-called fast cooled meteorites, in understanding key aspect of planetary formation and evolution based on their magnetic records preserved in nm-sized taenite grains.

1 Introduction

Most meteorites are believed to originate from small planetary bodies (< 500 km radius) formed within the first million years (Myr) of the solar system (McCoy et al., 2006). The existence of iron and stony-iron meteorites indicates that part of these bodies underwent large-scale differentiation (McCoy et al., 2006; Elkins-Tanton et al., 2011), possibly generating planetary magnetic fields by dynamo processes due to convection of molten metallic cores (Bryson et al., 2015; Nichols et al., 2016). Recent paleomagnetic studies in (stony-)iron meteorites suggest that these materials can preserve magnetic records of planetary fields generated by their parent bodies (Nichols et al., 2016; Maurel et al., 2020; Nichols et al., 2021). The cloudy zone (CZ), an intergrowth of tightly packed, nanometer-sized crystals (or islands) of taenite or tetrataenite embedded in a paramagnetic matrix (Blukis et al., 2017), is the most promising magnetic phase to have possibly recorded ancient magnetic activity in meteorites (Uehara et al., 2011). Recently developed novel techniques capable of selectively measuring magnetizations in a μm- to nm-scale (nanopaleomagnetism) allowed the first paleointensity estimates based on remanences recorded in the CZ to be made (Bryson et al., 2014b; Nichols et al., 2016). However, the lack in theoretical understanding of the CZ's recording process brings the current estimates into constant debate and revision (Berndt et al., 2016; Einsle et al., 2018; Maurel et al., 2019). Taenite islands that form in the CZ at $\lesssim 400$ °C upon cooling might undergo a phase transition to tetrataenite if the cooling of meteoritic metal is very slow ($< 150 - 2500$

°C/Myr, Nichols et al. (2020)). Tetrataenite ordering is suggested to critically affect the domain state of the island and the ability of CZ to maintain a stable magnetic recording (Einsle et al., 2018). Some key aspects of this ordering process, however, are still poorly constrained. Understanding which domain states form in nm-sized taenite islands in the CZ prior to tetrataenite ordering, their temporal stability and how they are modified during ordering (i.e., whether any paleomagnetic record in taenite can nonetheless be preserved through the phase transition), are all key for constraining the mechanism by which the CZ records magnetization in meteorites.

Recent micromagnetic models suggests that reliable magnetic recordings are created in the CZ through a series of modifications of the islands' domain states: first, taenite islands ($\sim$ 90 nm) form (unstable) single-vortex (SV) states for temperatures > 320 °C; second, SV states in taenite are gradually transformed into (also unstable) multi-domain (MD) states during tetrataenite ordering at 320 °C (Néel, 1964); finally, the MD states are transformed into stable SD states as tetrataenite ordering is complete (Einsle et al., 2018). In this model, the islands' magnetic domain states fundamentally change during ordering, thus suggesting that (i) stable SD magnetizations can be recorded only when tetrataenite orders in the CZ , and (ii) that any natural remanent magnetization (NRM) possibly carried by taenite former to the phase transition is lost during the ordering (Einsle et al., 2018). It has thus been widely accepted that reliable paleomagnetic records in meteorites are only possible in tetrataenite dominated CZs (Maurel et al., 2019; Nichols et al., 2020). Moreover, the formation of stable SD states in tetrataenite has been thought to occur only when its precursor taenite is large enough to form SV states (thus allowing the SV to MD to SD transitions to take place) (Nichols et al., 2020). This series of assumptions has thus restricted the number of meteorites that could, in principle, preserve paleomagnetic record. As a consequence, part of the fast cooled iron meteorites that experienced cooling rates of the order of $\sim$ 150 °C/Myr to $\sim$ 2500 °C/Myr, are usually disregarded as possible sources of paleomagnetic records. In these meteorites, the rapid cooling prevented both the growth in taenite islands (and the formation of SV states) as well as tetrataenite to order (Nichols et al., 2020). Fast cooled meteorites, particularly the IVAs, represent an important class of meteorites: they are fragments of planetary cores ejected during collisions between differentiated planetesimals (Asphaug, 2009), whose complete removal of the overlaid silicate mantle has exposed them to unusually rapid cooling. Recent planetary models have shown that mantle-stripped cores are likely to have generated self-exciting magnetic fields as they cooled (Neufeld et al., 2019). The forthcoming NASA mission Psyche will search for evidence of a past magnetic activity of the asteroid (16) Psyche (Elkins-Tanton et al., 2017), which is the largest ($\sim$ 180-km diameter) known metal-rich object ($\sim$ 30 to $\sim$ 60 vol.% metal, Elkins-Tanton et al. (2020)) in the main asteroid belt and believed to be an exposed metallic core of a mantle-stripped planetesimal. As a fast cooled metallic body, the (16) Psyche asteroid is likely to have CZs formed within its metallic materials and, hence, to share the same recording properties of most IVA meteorites. Assessing the paleomagnetic potential of the CZ in fast cooled materials is, therefore, a unique opportunity to obtain key constrains on important processes of planetary formation, e.g., top – down solidification process (Williams, 2009; Bryson et al., 2017), unconventional dynamo generation mechanisms (Hauck et al., 2006) and the importance of impacts on planetary formation (Asphaug, 2009; Asphaug & Reufer, 2014).

In this work, we address two major questions regarding the magnetic recording fidelity of iron meteorites: first, we investigate whether or not the taenite-containing CZs in fast cooled iron meteorites can nonetheless preserve stable natural remanent magnetizations over billion-year timescales, which would open the window into using this class of meteorites to study planetary core formation. Second, we discuss whether the CZ in other meteorites that experienced slower cooling rates, and which thus contain tetrataenite islands, can possibly retain any previous memory from the magnetization of taenite islands that existed prior to tetrataenite ordering. In this study, we approach these prob-

¹¹⁹ lems by carrying out extensive and systematic finite-element 3D micromagnetic simu-
¹²⁰ lations of taenite islands of various sizes and elongations and find that there is a wide
¹²¹ range of taenite island sizes that are thermally stable over billion-year timescales. Ad-
¹²² ditionally, we find a narrow size range where fine-grained tetrataenite may possibly re-
¹²³ tain a previous NRM inherited from the precursor taenite.

2 Methods

2.1 Islands sizes and shapes in the CZ

¹²⁶ Einsle et al. (2018) used a combination of different experimental methods to char-
¹²⁷ acterize the morphology of the CZ islands of the Tazewell IAB sLH iron meteorite. The
¹²⁸ results indicate the predominance of prolate triaxial grains, with elongation varying be-
¹²⁹ tween 0 % and 50 % in the intermediate (island sizes between ~ 60 nm and ~ 120 nm)
¹³⁰ and fine ($\lesssim 50$ nm) regions of the CZ. These are larger grains sizes than are reported in
¹³¹ the literature for fast cooled meteorites, where the island sizes range from ~ 12 nm to
¹³² ~ 32 nm (Table S4 in supplementary material). In this work we used finite-element mi-
¹³³ cromagnetic modelling to investigate the thermal stability of nm-sized taenite with sizes
¹³⁴ varying between 10 nm and 90 nm (in equivalent spherical volume diameter, ESVD), con-
¹³⁵ sidering two different grain geometries: (i) prolate spheroids and (ii) triaxial ellipsoids
¹³⁶ (Fig. 1). For both geometries the elongation is set along the [001] (easy-)direction of the
¹³⁷ cubic crystal structure of taenite. Percentage elongations varying between 0 % and 50
¹³⁸ % are considered, such that 0 % correspond to an equidimensional shape (in this study,
¹³⁹ a sphere) and 50 % correspond to a short to long axis ratio (e) equal to 0.5. The triax-
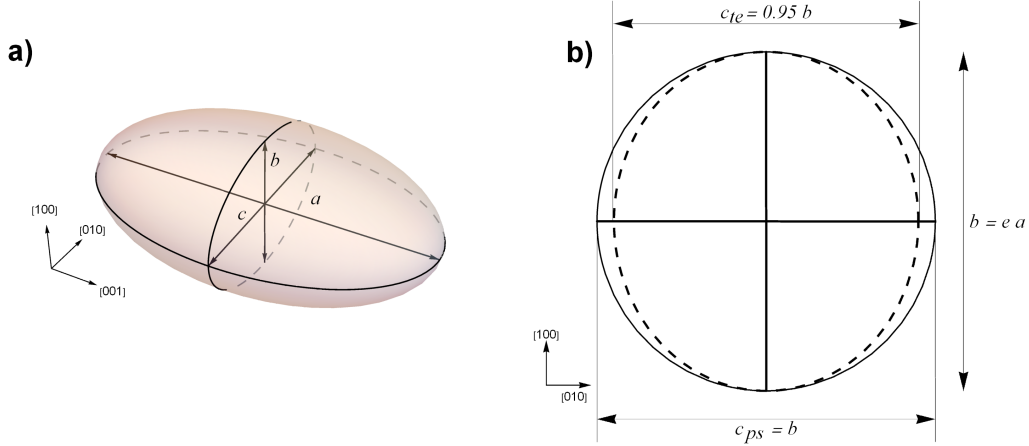¹⁴⁰ ial particles have an intermediate axis 5 % longer than the short axis (Fig. 1b).

Figure 1. Particle geometry. (a) An ellipsoidal geometry with axes length a, b and c. The spheroidal and triaxial ellipsoidal geometries used to describe the grain shapes investigated in this work are special cases based on this basic geometry. (b) Transversal view of the ellipsoidal shape depicted in (a). c_{ps}: minor axis width for prolate spheroids (which is equal in length to b); c_{te}: minor axis length for triaxial ellipsoids (= 0.95 b); e: elongation (= b/a).

2.2 Micromagnetic modeling

¹⁴² The finite-element micromagnetic modeling package MERRILL (Ó Conbhuí et al.,
¹⁴³ 2018) (version 1.5.2) is used to execute the simulations. For taenite, the room-temperature
¹⁴⁴ magnetic parameters used in this work are: saturation magnetization $M_s = 1{,}273$ kA/m,

145 anisotropy constant $K_1 = 1$ kJ/m^3 and exchange constant $A = 1.13\times10^{-11}$ J/m (Hÿtch
146 et al., 2003; Gehrmann, 2005). The meshed volumes describing the grains morphology
147 are created using the software Coreform Cubit (version 2021.11). The resolution of the
148 mesh of the particle is constrained to be less than the exchange length l (Rave et al., 1998):

$$l = \sqrt{\frac{2A}{\mu_0 M_s^2}}, \tag{1}$$

149 which is ~ 3 nm for taenite. However, for smaller grain sizes an even finer mesh reso-
150 lution was used: 1 nm for grains between 10 nm and 20 nm, 2 nm for grain sizes between
151 20 nm and 28 nm, and 3 nm for grain sizes > 30 nm.

152 The domain structure that minimizes the grain's internal energy is referred to as
153 a local energy minimum (LEM) state. We use the software Paraview (Ahrens et al., 2005)
154 to visualize the domain structure associated to the LEM states. To assess the thermal
155 stability of a particle, in principle all LEM states must be obtained. Although no com-
156 putational method guarantees that all LEM states can be determined, by performing a
157 large number of energy minimization seeded with initial random states for a given vol-
158 ume, it is possible to observe which LEM states are the most likely to occur. In this work,
159 for each grain shape, 100 minimizations are performed. From the LEM states it is pos-
160 sible to estimate the thermal stability of the magnetic state by calculating the energy
161 barriers (ΔE) between any two different domain states. The nudge-elastic-band (NEB)
162 method, implemented in MERRILL's micromagnetic routine, allows determination of
163 the minimal energy path over which a transition between two distinct LEM states is likely
164 to occur (Fabian & Shcherbakov, 2018). The energy barrier ΔE is then calculated as the
165 difference between the maximum energy value along the minimal path determined by
166 the NEB method and the energy of the initial LEM state. Based on ΔE the thermomag-
167 netic stability of a domain state is estimated by calculating the relaxation time associ-
168 ated with the transition using the Néel-Arrhenius equation (Néel, 1949):

$$\tau = \tau_0 \exp\left(\frac{\Delta E}{k_B T}\right), \tag{2}$$

169 with $\tau_0 = 10^{-9}$ s the atomic attempt time (Berndt et al., 2015), k_B the Boltzmann con-
170 stant and T the temperature.

3 Results

3.1 Domain states in nm-sized taenite

173 Micromagnetic results revealed a gradual change in taenite's domain state, from
174 uniform to non-uniform, as a function of grain size. Both grain shapes (spheroidal and
175 triaxial ellipsoidal) exhibit uniform SD states magnetized along the long axis for smaller
176 sizes Fig. 2a (see supplementary material, Fig. S1), while larger grains display non-uniform
177 domain states. We observed three different non-SD structures: (i) long-axis-aligned-SV
178 (LSV), in which a magnetic vortex is aligned with the long axis of the grain (Fig. 2b and
179 Fig. S1 in supplementary material), (ii) short-axis-aligned-SV (SSV), in which the vor-
180 tex core is aligned with the short axis (Fig.2c,d) and (iii) "twisted-SV" (TSV) states,
181 in which the vortex core does not follow a straight line (Fig. 2e,f). The latter is possi-
182 bly a transitional state from a SV to a multi-vortex state.

183 The critical grain sizes that mark transitions between distinct domain structures
184 were obtained from size hysteresis loops (Fig. S1 in the supplementary material) (Ó Conbhuí
185 et al., 2018). There are three critical grain sizes: The transition from SV to LSV (d_{LSV}^{SD}),
186 from LSV to SSV (d_{SSV}^{LSV}), and from SSV to TSV (d_{TSV}^{SSV}). This sequence of domain states
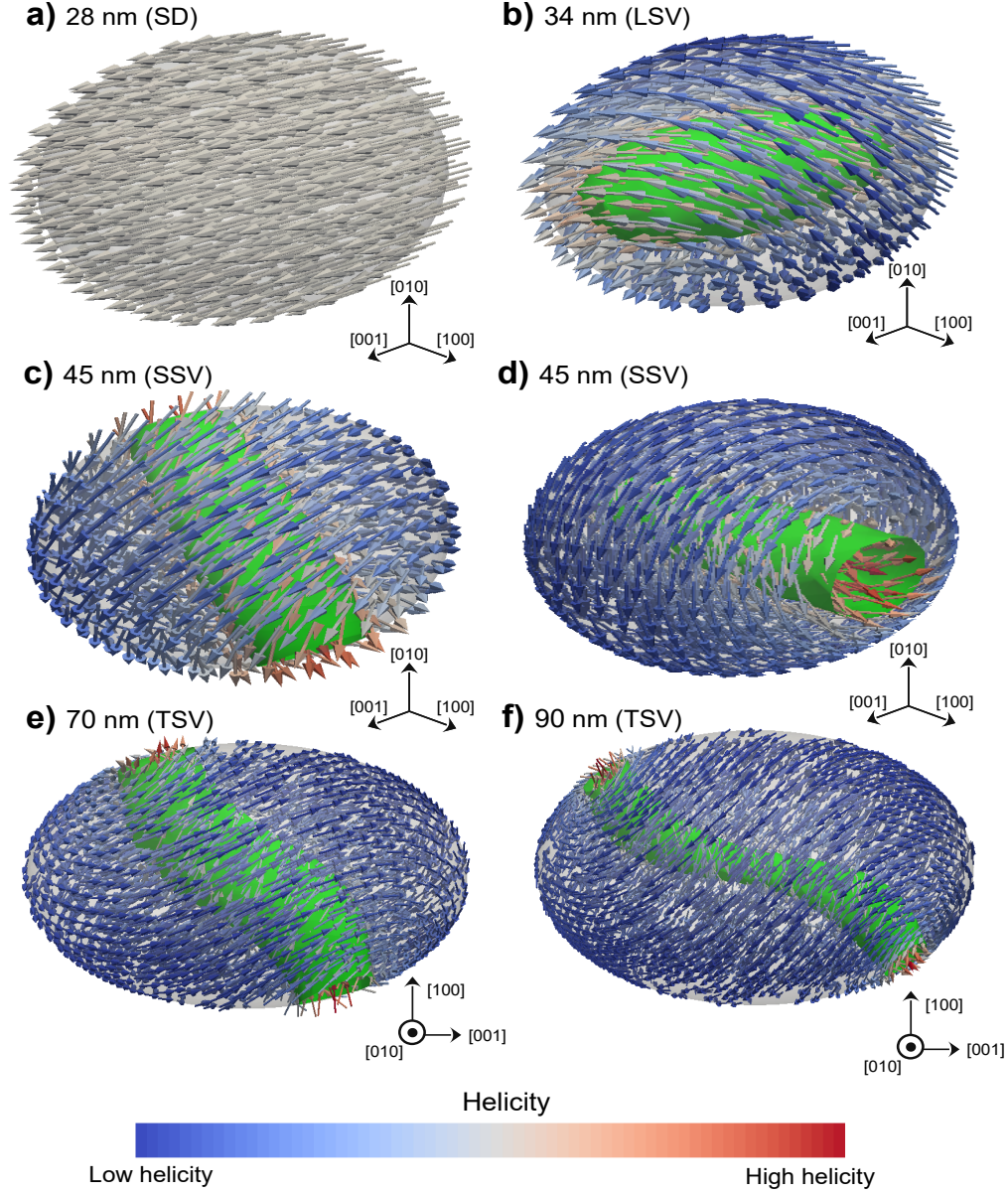
Figure 2. Magnetic domain structures for 30% elongated, spheroidal taenite grains with different sizes. (a) SD state (28 nm); (b) LSV state (34 nm); (c, d): two different SSV states observed in a 45 nm sized grain; (e) TSV state (70 nm); (f) TSV state (90 nm). The green surfaces are helicity iso-surfaces. The same domain states and size thresholds were observed in triaxial grains (see Table S1).

(SD to LSV to SSV to TSV) was observed in both spheroidal and triaxial grains, and the critical grain sizes were virtually identical (Table S4 in supplementary material). However, grains in the SSV to TSV range show an important difference in behaviour depending on the spheroidal/triaxial shape: while triaxial grains have four distinct stable domain states (each differing only in the sign of the total magnetic moment and the sign of the total vorticity), spheroidal grain's vortex cores (and therefore, magnetic moment vectors) are free to rotate about the elongation axis (SSV), or about a certain solid angle around the elongation axis (TSV) (Figure S3 in supplementary material). This effect is due to the rotational symmetry of spheroidal grains, together with the extremely weak magnetocrystalline anisotropy of taenite.

3.2 Energy barriers

NEB results indicate two mechanisms of magnetization reversal in the SD size range: (*i*) coherent rotation (CR), in which the SD structure as a whole is rotated coherently, and (*ii*) via vortex nucleation (VN), which involves the nucleation of a magnetic vortex through the minimized energy path (usually a SSV state, Fig. 2d), rotation of the vortex structure, and reestablishment of a uniform state. CR is observed in grain sizes $< d_{LSV}^{SD}$, while reversals via VN are observed in the proximity of uniform to non-uniform transition (i.e., grains sizes $\lesssim d_{LSV}^{SD}$). Energy barriers associated to CR reversals are larger than those that occurs via VN (Fig. 3a).

There are narrow transition zones in the proximity of d_{LSV}^{SD}, d_{SSV}^{LSV}, and d_{TSV}^{SSV} of around ∼4 to ∼12 nm, where more than one domain structure can occur (see Fig. S1 in supplementary material). For instance, in the proximity of d_{LSV}^{SD}, both SD (with higher internal energy) and LSV (with lower internal energy) states are observed within the micromagnetic solutions; in these cases, we used only the lowest energy domain states to calculate energy barriers. Transitions between LSV states of opposite magnetic moment (Fig. 3e,k) occur through a process similar to coherent rotation, in which the whole vortex structure is rotated coherently (structure coherent rotation, Nagy et al. (2017))

SSV and TSV states in spheroidal grains can occur in any direction about a solid angle, without any effective energy barrier between these different states. In triaxial grains, however, the small deformation about the intermediate axis is sufficient to create an energy barrier of a magnitude comparable or higher than that of LSV transitions (Fig. 3 and S3 in supplementary materials).

3.3 Domain state stability

For spheroidal grains, the smallest SD grains are superparamagnetic, while above ∼ 14 nm most are stable over geological time scales (Fig. 4). Up to the 40–50 nm (depending on elongation), particles are LSV and almost all are stable. Above this range, spheroidal particles become SSV/TSV, and hence have zero energy barrier, allowing them to freely rotate about a solid angle – their relaxation time therefore approaches zero. Triaxial grains, on the other hand (while showing the same behaviour for small sizes), do not have this rotational symmetry: Therefore, the larger SSV/TSV grains (starting from 30-50 nm depending on elongation), have increasingly larger energy barriers, such that – apart from a narrow low-stability trough around 30-50 nm – particles become very stable again.

4 Discussion

4.1 Paleomagnetic potential of fast cooled iron meteorites

Micromagnetic results presented in this work indicate that taenite forms SV states in grain sizes $\gtrsim$ 34 nm (depending on elongation), which is in agreement with previous
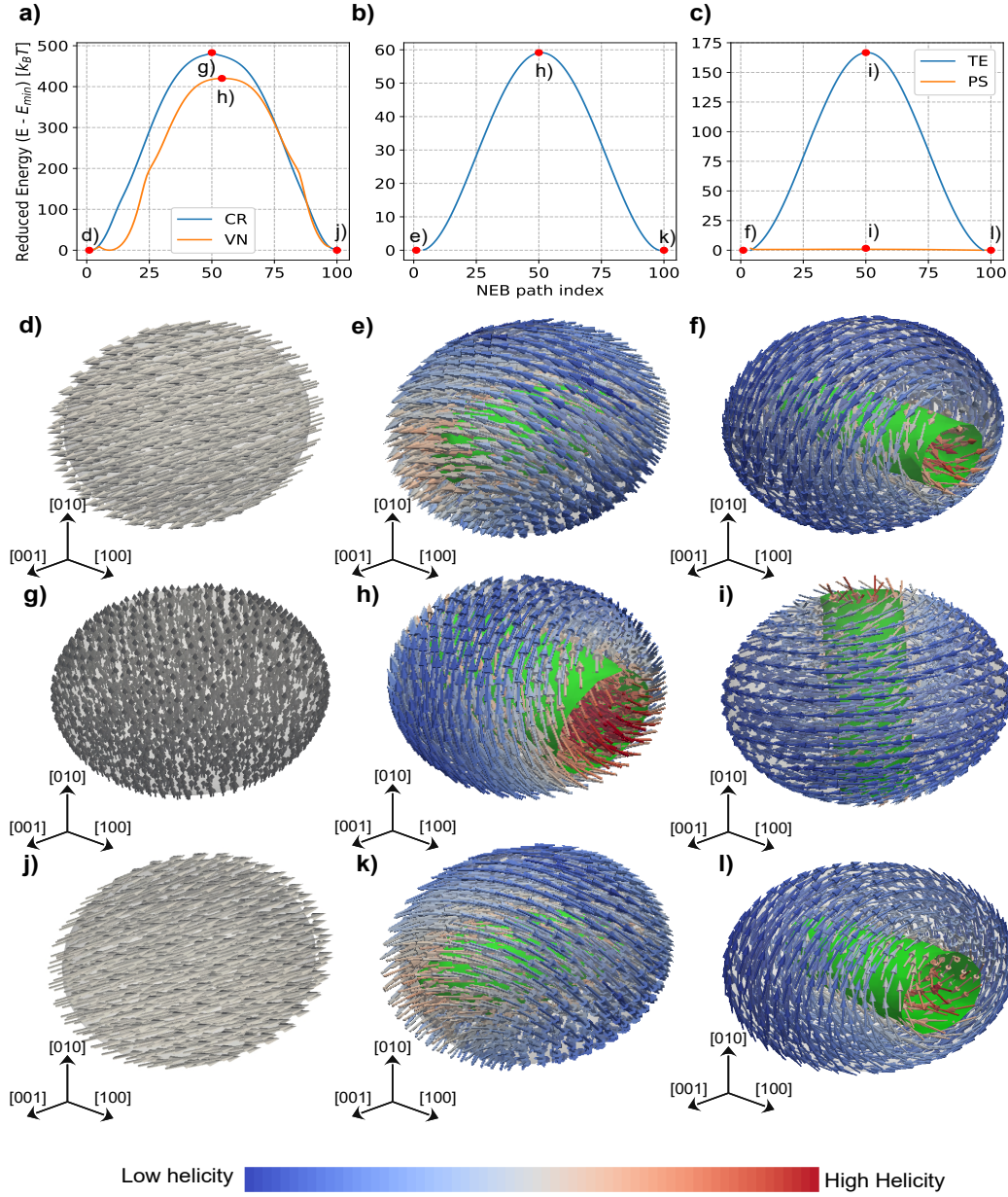
Figure 3. Transitions between different domain state in shperoidal taenite grains. (a–c) Energy barriers, (d–l) domain states of ground state, maximum energy state, and opposite ground state. *Left column*: SD–SD transition through coherent rotation (CR); *centre column*: LSV–LSV transition; *right column*: SSV–SSV transition for a triaxial ellipsoid (TE, blue line) and a prolate spheroid (PS, orange line). Also in (a): some larger SD states transition through vortex nucleation (VN, orange line), through a sequence given by Figs (d)-(h)-(j).
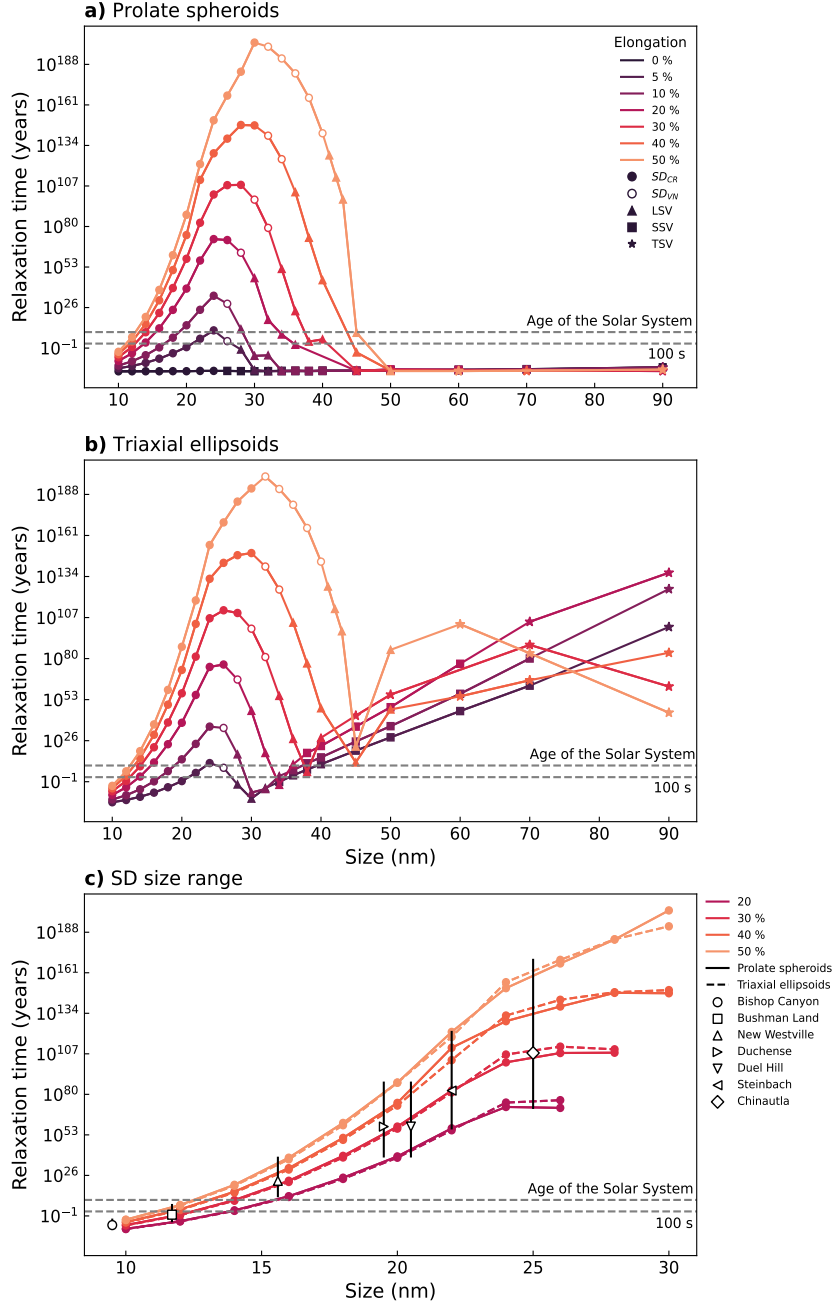
Figure 4. Thermal stability / relaxation times of (a) spheroidal, (b) triaxial taenite grains and (c) within the SD size range for both shapes. In (c), hollow (circle, square, triangles and diamond) symbols are the relaxation times calculated for island sizes of some IVA meteorites. We consider particles with 78 % of the island sizes observed experimentally, as this is suggested to be the approximate size of the islands at 320 °C (Maurel et al., 2019). Lines correspond to the different elongations (in %). The bars correspond to the highest (50 %) and lowest (20 %) elongations, respectively, used to calculate the relaxation times for the IVAs. Spheres, triangles, squares and pentagram represent the sizes in which SD-SD, LSV-LSV, SSV-SSV and TSV-TSV transitions were used to calculate relaxation times, respectively. For SD states, transitions can occur through coherent roation (CR) or via vortex nucleation (VN).

numerical models (Einsle et al., 2018). Our results also show, however, that there is a size range, from ~14 nm to ~34 nm, for which taenite forms stable SD states (Fig. 4). Previous works suggested that taenite islands in the CZ tend to occur in vortex states and only form SD states upon ordering to tetrataenite under extremely slow cooling (Einsle et al., 2018). The existence of a SD range in nm-sized taenite grains is important for both slowly cooled meteorites (as discussed in the next section), and for fast cooled meteorites: rapid cooling of a meteorite (150 to 2500 °C/Myr, Nichols et al., 2020), such as the IVAs, both prevents the islands to grow bigger, and prevents taenite from ordering to tetrataenite; they are, therefore, believed to preserve fine-grained (< 50 nm), taenite-containing CZs (Nichols et al., 2020). It was previously assumed that the low coercivity of bulk taenite implied low thermal stability, making fast cooled meteorites poor candidates for paleomagnetic recorders (Bryson et al., 2014b; Einsle et al., 2018; Nichols et al., 2020). Our results suggest otherwise: We have shown here that taenite-containing CZs in fast cooled meteorites are stable over billion-year timescales, and are thus good candidates to provide reliable paleomagnetic records of ancient dynamo activity in meteorites. Based on experimentally measured island sizes of IVA meteorites (Yang et al., 1997; Goldstein et al., 2009), we show that most of them are likely to have formed stable SD taenite grains at $\gtrsim$320 °C (Fig. 4c). Note that fast cooling for iron meteorites is still at sufficiently slow rates (see Table S4 in supplementary material), that we can expect the change in temperature to be slower than the increase in grain size with respect to controlling the blocking of the grains' magnetization. Therefore, we suggest that fast cooled meteorites are likely to preserve stable crystallization remanent magnetizations (CRMs) in their CZs over billion-year timescales. This opens the possibility of assessing ancient dynamo activity based on record preserved in taenite-containing CZs of fast cooled meteorites.

4.2 Taenite-inherited remanence in tetrataenite-containing meteorites

Tetrataenite islands in the CZ form through the ordering of disordered taenite islands (Maurel et al., 2019). Our results indicate that most IVA meteorites are likely to have formed stable SD taenite grains at 320 °C. Fast cooled meteorites contain predominantly fine-grained CZ islands (< 50 nm) and may either avoid ordering to tetrataenite, or in some cases partially or completely order to tetrataenite (e.g., IVA Steinbach, Bryson et al. (2014a)). In fast cooled meteorites that form tetrataenite in the CZ, the chemical ordering is likely to take place from an underlying SD state of its precursor taenite – at least for the finer grain sizes. This is fundamentally different to recent numerical models (Einsle et al., 2018) suggesting that large (> 60 nm) SV taenite grains undergo a series of domain modifications during tetrataenite ordering that leads to a complete loss of any taenite-precursor magnetization. While not explicitly shown by our model, it strongly suggests that a precursor SD taenite island would retain an identical or similar SD state upon the phase transition to SD tetrataenite.

Note, however, that during chemical ordering (below 320 °C), tetrataenite aligns its uniaxial anisotropy axis along one of the $\langle 100 \rangle$ directions of the underlying cubic structure of taenite (Clarke & Scott, 1980; Bryson et al., 2014a; Einsle et al., 2018), such that the tetrataenite magnetocrystalline easy axis would not necessarily correspond to the taenite magnetostatic easy (i.e., elongation) axis, which might modify the domain state. Tetrataenite does, however, tend to align its anisotropy axis in the direction of the external field (Bryson et al., 2014a) – although it is conceivable that the internal magnetization of the precursor taenite also influences the orientation of tetrataenite's anisotropy axis (and, hence, its easy-directions of magnetization), which would then reinforce the precursor SD magnetization. It has long been suggested that fine-grained tetrataenite might inherit the domain state of its precursor taenite (Wasilewski, 1988) (similar to remanence inheritance upon maghemitization), and our simulations add weight to this hypothesis for the SD size range. In fast cooled meteorites, the preservation of domain states during tetrataenite ordering would represent a new mechanism remanence recording by the CZ, distinct from the domain modifications proposed by Einsle et al. (2018).

It is currently assumed that only SD tetrataenite can preserve reliable records in meteoritic CZs, implying that the temperature at which the islands' magnetic moment are blocked is, thus, the temperature at which tetrataenite orders (i.e., 320 °C). However, our results show that taenite-containing CZs are likely to record stable CRMs as taenite islands surpass their blocking volume and possibly inherit the uniform state on subsequent tetrataenite ordering. Taenite-inherited remanences in tetrataenite-containing CZs suggests, thus, that in fast cooled meteorites, the islands' bloocking temperature is not 320°C as usually assumed (Bryson et al., 2014a; Maurel et al., 2019; Nichols et al., 2020), but is instead somewhere between ∼400 °C (i.e., the temperature at which taenite islands form in the CZ) and 320 °C. Based on the reported cooling rate for fast cooled meteorites (see Table S4 in supplementary material), this could translate to a temporal discrepancy of up to ∼10^5 years in the timing of magnetic recording: any NRM preserved by tetrataenite islands (and measured nowadays), could have been recorded by stable SD states in taenite islands (as a CRM) up to ∼ 10^5 years before the ordering started. Larger, SV taenite-precursor islands, may, however, have been completely reset upon ordering to tetrataenite, such that these tetrataenite islands would have recorded a new phase-transition-remanent-magnetization ∼ 10^5 years later. Therefore, fast cooled iron meteorites, may in-fact carry two distinct remanent magnetizations: one recorded by the precursor taenite between 320 and 400 °C, and a second one recorded ∼ 10^5 years later through the phase transition to tetrataenite. In fact, small planetesimals usually have short-lived thermomagnetic activity, so time lapses of the order of ∼10^5 years might encompasses completely distinct stages (onset and quiescence of a dynamo, for instance, Bryson et al. (2017)) of their magnetic history.

5 Conclusions

There are two major implications for paleomagnetic recording in fast cooled meteorites that results from this work: First, we showed that, contrary to what is commonly assumed, most nm-sized taenite grains can preserve stable magnetization states over billion-yeaers timescales, indicating that taenite-containing CZs can provide reliable paleomagnetic records of ancient activity in meteorites. This gives a unique opportunity of investigating key aspect of core formation and dynamo generation based on magnetic records preserved in these meteorites. Second, we suggest that tetrataenite-containing CZs in some fast cooled might preserve a taenite-inherited remanence, recorded on growth of taenite islands and inherited by tetrataenite as it orders. The preservation of stable SD taenite states through tetrataenite ordering would impact the timing of paleomagnetic record: NRMs preserved by tetrataenite islands (and measured nowadays) might reflect an (up to ∼ 10^5 years) older CRM, recorded as taenite islands grew bigger and preserved through subsequente tetrataenite ordering. A more constrained blocking estimate requires, however, the knowledge of the temperature-dependence of (tetra)taenite's properties, as well as the understanding of how the ordering affects the island's domain states – both effects are still poorly understood. Undestanding these key aspects can provide additional constrains on the timing of magnetic recording in meteoritic CZs, which is essential to obtain meaningful estimates of paleomagnetic activity in meteorites.

6 Open Research

All results reported here were generated using the open source micromagnetic modeling code MERRILL (Conbhuí et al., 2018). A complete guide to installation and use of MERRILL is described here: `https://blogs.ed.ac.uk/rockmag`. The data required to reproduce our results (MERRILL script and geometries) is available at `https://github.com/devienne/taenite_tetrataenite`.

Acknowledgments

References

Ahrens, J., Geveci, B., & Law, C. (2005). Paraview: An end-user tool for large-data visualization. In *Visualization handbook.* Amsterdam, the Netherlands: Elsevier.

Asphaug, E. (2009). Growth and evolution of asteroids. *Annual Review of Earth and Planetary Sciences*, *37*(1), 413-448. doi: 10.1146/annurev.earth.36.031207.124214

Asphaug, E., & Reufer, A. (2014). Mercury and other iron-rich planetary bodies as relics of inefficient accretion. *Nature Geoscience*, *7*, 564-568. doi: 10.1038/ngeo2189

Berndt, T., Muxworthy, A. R., & Fabian, K. (2016). Does size matter? statistical limits of paleomagnetic field reconstruction from small rock specimens. *Journal of Geophysical Research: Solid Earth*, *121*(1), 15-26. doi: https://doi.org/10.1002/2015JB012441

Berndt, T., Muxworthy, A. R., & Paterson, G. A. (2015). Determining the magnetic attempt time τ_0, its temperature dependence, and the grain size distribution from magnetic viscosity measurements. *Journal of Geophysical Research: Solid Earth*, *120*(11), 7322-7336. doi: https://doi.org/10.1002/2015JB012283

Blukis, R., Rüffer, R., Chumakov, A. I., & Harrison, R. J. (2017). A high spatial resolution synchrotron mössbauer study of the tazewell IIICD and esquel pallasite meteorites. *Meteoritics & Planetary Science*, *52*(5), 925-936. doi: https://doi.org/10.1111/maps.12841

Bryson, J. F., Church, N. S., Kasama, T., & Harrison, R. J. (2014b). Nanomagnetic intergrowths in fe-ni meteoritic metal: The potential for time-resolved records of planetesimal dynamo fields. *Earth and Planetary Science Letters*, *388*, 237-248. doi: 10.1016/j.epsl.2013.12.004

Bryson, J. F., Herrero-Albillos, J., Kronast, F., Ghidini, M., Redfern, S. A., Van der Laan, G., & Harrison, R. J. (2014a). Nanopaleomagnetism of meteoritic fe-ni studied using x-ray photoemission electron microscopy. *Earth and Planetary Science Letters*, *396*, 125–133. doi: 10.1016/j.epsl.2014.04.016

Bryson, J. F., Nichols, C. I., Herrero-Albillos, J., Kronast, F., Kasama, T., Alimadadi, H., ... Harrison, R. J. (2015). Long-lived magnetism from solidification-driven convection on the pallasite parent body. *Nature*, *517*(7535), 472–475. doi: 10.1038/nature14114

Bryson, J. F., Weiss, B. P., Harrison, R. J., Herrero-Albillos, J., & Kronast, F. (2017). Paleomagnetic evidence for dynamo activity driven by inward crystallisation of a metallic asteroid. *Earth and Planetary Science Letters*, *472*, 152–163. doi: 10.1016/j.epsl.2017.05.026

Clarke, R., & Scott, E. (1980). - Feni, a New Mineral in Meteorites. *American Mineralogist*, *65*(1959), 624–630.

Conbhuí, P., Williams, W., Fabian, K., Ridley, P., Nagy, L., & Muxworthy, A. R. (2018). Merrill: Micromagnetic earth related robust interpreted language laboratory. *Geochemistry, Geophysics, Geosystems*, *19*(4), 1080–1106. doi: 10.1002/2017GC007279

Einsle, J. F., Eggeman, A. S., Martineau, B. H., Saghi, Z., Collins, S. M., Blukis, R.,

... Harrison, R. J. (2018). Nanomagnetic properties of the meteorite cloudy zone. *Proceedings of the National Academy of Sciences*, *115*(49), E11436– E11445. doi: 10.1073/pnas.1809378115

Elkins-Tanton, L. T., Asphaug, E., Bell, J. F. I., Bercovici, D., Bills, B. G., & Binzel, R. P. e. a. (2017). Asteroid (16) psyche: Visiting a metal world. *Lunar Planet. Sci. Conf*, *48*, abstract 1718.

Elkins-Tanton, L. T., Asphaug, E., Bell III, J. F., Bercovici, H., Bills, B., & Binzel, R. e. a. (2020). Observations, meteorites, and models: A preflight assessment of the composition and formation of (16) psyche. *Journal of Geophysical Research: Planets*, *125*(3), e2019JE006296. doi: https://doi.org/10.1029/ 2019JE006296

Elkins-Tanton, L. T., Weiss, B. P., & Zuber, M. T. (2011). Chondrites as samples of differentiated planetesimals. *Earth and Planetary Science Letters*, *305*(1-2), 1– 10. doi: 10.1016/j.epsl.2011.03.010

Fabian, K., & Shcherbakov, V. P. (2018). Energy barriers in three-dimensional micromagnetic models and the physics of thermoviscous magnetization. *Geophysical Journal International*, *215*(1), 314-324. doi: 10.1093/gji/ggy285

Gehrmann, B. (2005). Nickel–iron alloys with special soft magnetic properties for specific applications. *Journal of magnetism and magnetic materials*, *4*, 290-291.

Goldstein, J. I., Scott, E. R., & Chabot, N. L. (2009). Iron meteorites: Crystallization, thermal history, parent bodies, and origin. *Chemie der Erde*, *69*(4), 293– 325. doi: 10.1016/j.chemer.2009.01.002

Hauck, S. A., Aurnou, J. M., & Dombard, A. J. (2006). Sulfur's impact on core evolution and magnetic field generation on ganymede. *Journal of Geophysical Research: Planets*, *111*, E09008. doi: https://doi.org/10.1029/2005JE002557

Hÿtch, M. J., Dunin-Borkowski, R. E., Scheinfein, M. R., Moulin, J., Duhamel, C., Mazaleyrat, F., & Champion, Y. (2003). Vortex flux channeling in magnetic nanoparticle chains. *Physical Review Letters*, *91*(25), 257207. doi: https://doi.org/10.1103/PhysRevLett.91.257207

Maurel, C., Bryson, J. F. J., Lyons, R. J., Ball, M. R., Chopdekar, R. V., Scholl, A., ... Weiss, B. P. (2020). Meteorite evidence for partial differentiation and protracted accretion of planetesimals. *Science Advances*, *1*, 1–10.

Maurel, C., Weiss, B. P., & Bryson, J. F. (2019). Meteorite cloudy zone formation as a quantitative indicator of paleomagnetic field intensities and cooling rates on planetesimals. *Earth and Planetary Science Letters*, *513*, 166–175. doi: 10.1016/j.epsl.2019.02.027

McCoy, T., Mittlefehldt, D., & Wilson, L. (2006). Asteroid differentiation. In *Meteorites and the early solar system II* (p. 733-745). Cambridge University Press.

Nagy, L., Williams, W., Muxworthy, A. R., Fabian, K., Almeida, T. P., Conbhuí, P. Ó., & Shcherbakov, V. P. (2017). Stability of equidimensional pseudo-single-domain magnetite over billion-year timescales. *Proceedings of the National Academy of Sciences*, *114*(39), 10356-10360. doi: 10.1073/pnas.1708344114

Néel, L. (1949). Théorie du trainage magnétique des ferromagnétiques en grains fins avec application aux terres cuites. *Annales de Géophysique*, 99–136.

Néel, L. (1964). Magnetic properties of nickel–iron alloys bombarded by neutrons in a magnetic field. *Journal of Applied Physics*, 873–876.

Neufeld, J. A., Bryson, J. F., & Nimmo, F. (2019). The top-down solidification of iron asteroids driving dynamo evolution. *Journal of Geophysical Research: Planets*, *124*(5), 1331–1356. doi: 10.1029/2018JE005900

Nichols, C. I., Bryson, J. F., Cottrell, R. D., Fu, R. R., Harrison, R. J., Herrero-Albillos, J., ... Weiss, B. P. (2021). A time-resolved paleomagnetic record of main group pallasites: Evidence for a large-cored, thin-mantled parent body. *Journal of Geophysical Research: Planets*, *126*(7), e2021JE006900. doi: https://doi.org/10.1029/2021JE006900

Nichols, C. I., Bryson, J. F., Herrero-Albillos, J., Kronast, F., Nimmo, F., & Harrison, R. J. (2016). Pallasite paleomagnetism: Quiescence of a core dynamo. *Earth and Planetary Science Letters*, *441*, 103–112. doi: 10.1016/j.epsl.2016.02.037

Nichols, C. I., Bryson, J. F. J., Blukis, R., Herrero-Albillos, J., Kronast, F., Rüffer, R., ... Harrison, R. J. (2020). Variations in the magnetic properties of meteoritic cloudy zone. *Geochemistry, Geophysics, Geosystems*, *21*(2), e2019GC008798. doi: https://doi.org/10.1029/2019GC008798

Rave, W., Fabian, K., & Hubert, A. (1998). Magnetic states of small cubic particles with uniaxial anisotropy. *Journal of Magnetism and Magnetic Materials*, *190*(3), 332-348. doi: https://doi.org/10.1016/S0304-8853(98)00328-X

Uehara, M., Gattacceca, J., Leroux, H., Jacob, D., & Van Der Beek, C. J. (2011). Magnetic microstructures of metal grains in equilibrated ordinary chondrites and implications for paleomagnetism of meteorites. *Earth and Planetary Science Letters*, *306*(3-4), 241–252. doi: 10.1016/j.epsl.2011.04.008

Wasilewski, P. (1988). Magnetic characterization of the new magnetic mineral tetrataenite and its contrast with isochemical taenite. *Physics of the Earth and Planetary Interiors*, *52*(1-2), 150–158. doi: 10.1016/0031-9201(88)90063-5

Williams, Q. (2009). Bottom-up versus top-down solidification of the cores of small solar system bodies: Constraints on paradoxical cores. *Earth and Planetary Science Letters*, *284*(3), 564-569. doi: https://doi.org/10.1016/j.epsl.2009.05.019

Yang, C., Williams, D., & Goldstein, J. (1997). Low-temperature phase decomposition in metal from iron, stony-iron, and stony meteorites. *Geochimica et Cosmochimica Acta*, *61*(14), 2943–2956. doi: 10.1016/S0016-7037(97)00132-4

Ó Conbhuí, P., Williams, W., Fabian, K., Ridley, P., Nagy, L., & Muxworthy, A. R. (2018). Merrill: Micromagnetic earth related robust interpreted language laboratory. *Geochemistry, Geophysics, Geosystems*, *19*(4), 1080-1106. doi: https://doi.org/10.1002/2017GC007279